NASA CR-66844

GARRETT

AIRESEARCH MANUFACTURING COMPANY

Los Angeles, California

HYPERSONIC RESEARCH ENGINE PROJECT - PHASE IIA
NASA CONTRACT NO. NAS1-6666
COOLANT PASSAGE FIN HEAT TRANSFER
AND PRESSURE DROP PERFORMANCE

Document No. AP-69-5348

Number of pages 28

Original date 7 August 1969

Prepared by E. M. Walters

Edited by L. F. Jilly

Approved by Henry J. Lopez
HRE Program Manager

ABSTRACT

Procedures and results of tests of the Hypersonic Research Engine (HRE) cowl leading edge configurations designed for Mach number 8 flight, are described. Two 0.030 inch leading edge radius configurations, one designed for hydrogen coolant flow parallel and one designed for hydrogen coolant flow perpendicular to the leading edge were tested to determine heat transfer performance, thermal cycle performance and coolant flow distribution. Both hot gas and radiant heating tests were performed. Results indicate the thermal performance and 100 cycles 10 hour life requirements were met.

CONTENTS

ILLUSTRATIONS

TABLES

NOMENCLATURE

A	flow area
A_D	duct flow area
A_f	fin heat transfer area
A_T	total heat transfer area
A_w	wall area
b	fin height between plates
C_p	specific heat at constant pressure
d	hydraulic diameter
f	Fanning friction factor
g	conversion factor 32.17 $lb_M ft/lb_F sec^2$
h	heat transfer coefficient
j	Colburn heat transfer factor
K	area change pressure loss coefficient
k	thermal conductivity
L	fluid flow length for pressure drop
L_f	effective fin length
L_o	fin offset length (uninterrupted length parallel to flow)
M	Mach number
N	number of fins per inch of flow width
P	pressure
Pr	Prandtl number
Q	heat transfer rate
R	gas constant
Re	Reynolds number

St	Stanton number
T	temperature
t	fin thickness
t_w	effective wall thickness
UA	overall thermal conductance
W	weight flow rate
η_f	fin heat transfer surface effectiveness
η_o	overall heat transfer surface effectiveness
μ	dynamic viscosity
ρ	density

Subscripts

A	air
f	fin
M	log mean average
w	water
1	inlet
2	outlet

I. INTRODUCTION

1.1 PURPOSE AND SCOPE

Tests to determine heat transfer and pressure drop performance of the brazed, rectangular offset, plate-fin cooling passage geometry were performed to verify the data used in design of the HRE cooling passages. The pressure drop is important for specification of the cooling system inlet pressure, and of the pressure containment capability of the entire cooling system, especially the inlet manifolds. Fin heat transfer performance controls the cross-section temperature difference which results at the local heating conditions and, therefore, controls the low cycle fatigue life of the engine cooling jackets.

The two principle fin configurations used in the regeneratively cooled surfaces of the HRE were tested. These surfaces were used where the heat fluxes are highest and contribute a significant fraction of the overall pressure drop. They have geometries which are different from those previously tested by AiResearch and others. The minimum Reynolds number at the Mach 8, 88,000-ft altitude design point is above the maximum test-Reynolds number previously reported for similar fins. The Hastelloy X material used for fin fabrication also produced particular effects on the fin geometry, as related to fin-forming and the existence of burrs. A third fin geometry used only on the forward part of the inlet spike was not tested because (1) the geometry was unchanged from that previously tested by AiResearch, (2) the heat flux and cross section temperature differences on the spike produced minimum thermal fatigue problems, and (3) the pressure drop in this section was moderate.

1.2 APPLICABLE DOCUMENTS

This section not applicable to this report.

2. DESCRIPTION OF TEST UNITS

The two test units were designed and built from Hastelloy X, and incorporated the two most generally used fin geometries in the HRE. Only one test unit is shown in Figure 2-1, as both units were identical in external configuration. The vertical tubes are for airflow through the two rows of test fins in each unit. The horizontal tubes are for water flow through one row of known-performance fins in each unit. Static pressure-sensing tubes and thermocouples for both fluids are depicted.

An edge view of the test specimen and known fins before attachment of manifolds is shown in Figure 2-2. Nominal fin geometry is noted. A cross-section through the air manifolds in Figure 2-3 shows the location of pressure and temperature sensors and the straight-duct sections in the manifolds. The layers of fin were separated and bounded on external surfaces by 24-mil-thick Hastelloy X plates and brazed with Palniro-1 alloy. The flow dimensions and other geometric characteristics of both test units are shown in Table 2-1.

An X-ray of both test units revealed that fins near the edge of one row of test fins in both units were blocked by braze alloy. This observation was confirmed by examination of the sectioned units. The braze-blockage width and the reductions in flow area and heat transfer area are noted in Table 2-1.

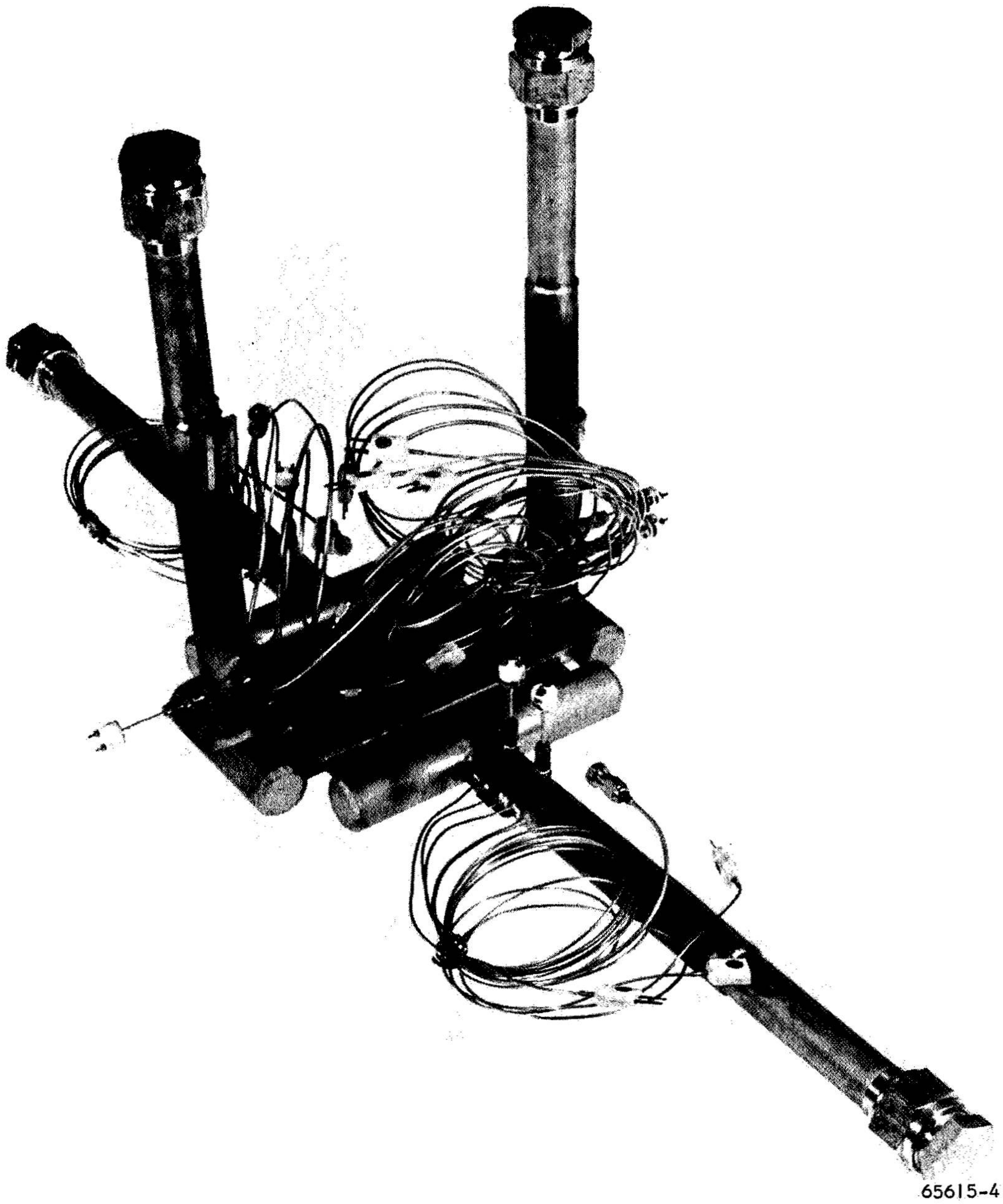

Figure 2-1. Cooled-Surface Performance Test Unit

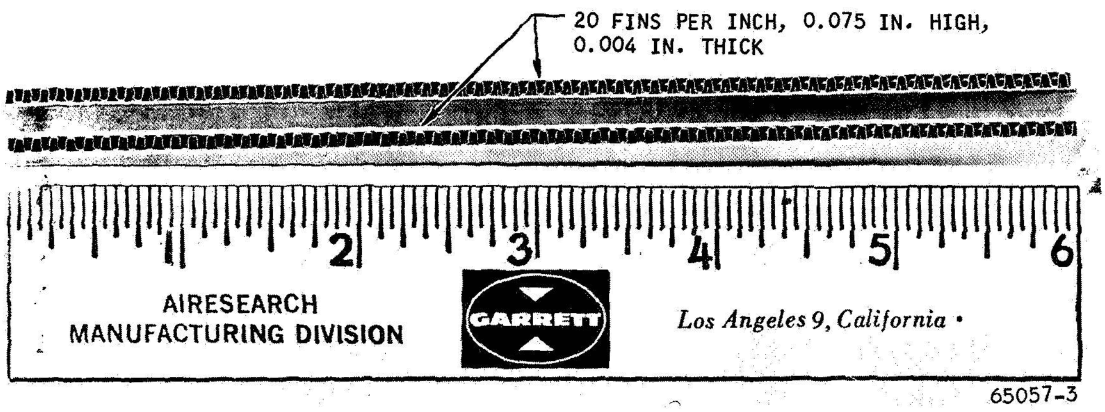

a. KNOWN FIN

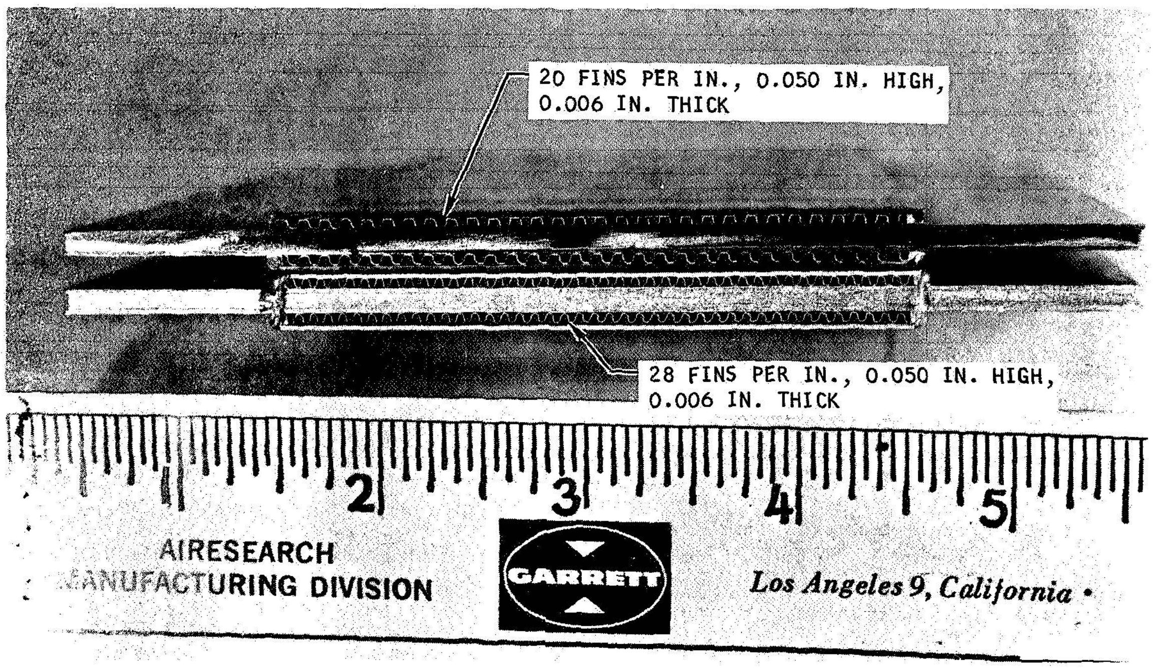

b. TEST FINS

F-11096

Figure 2-2. Heat Exchanger Test Fins and Known Fins

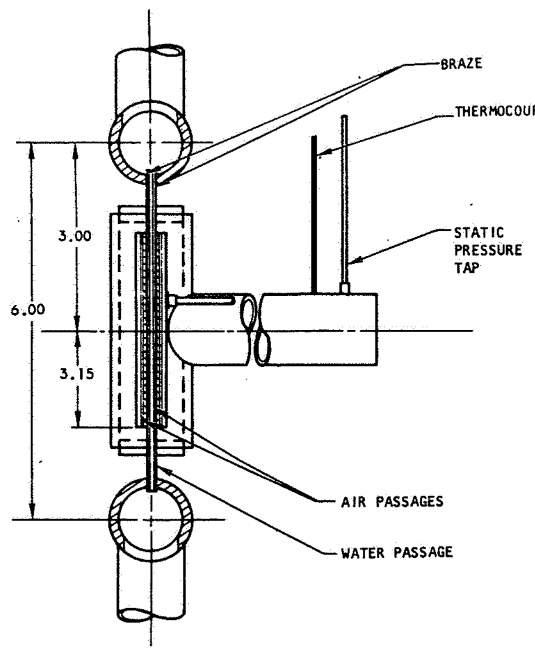

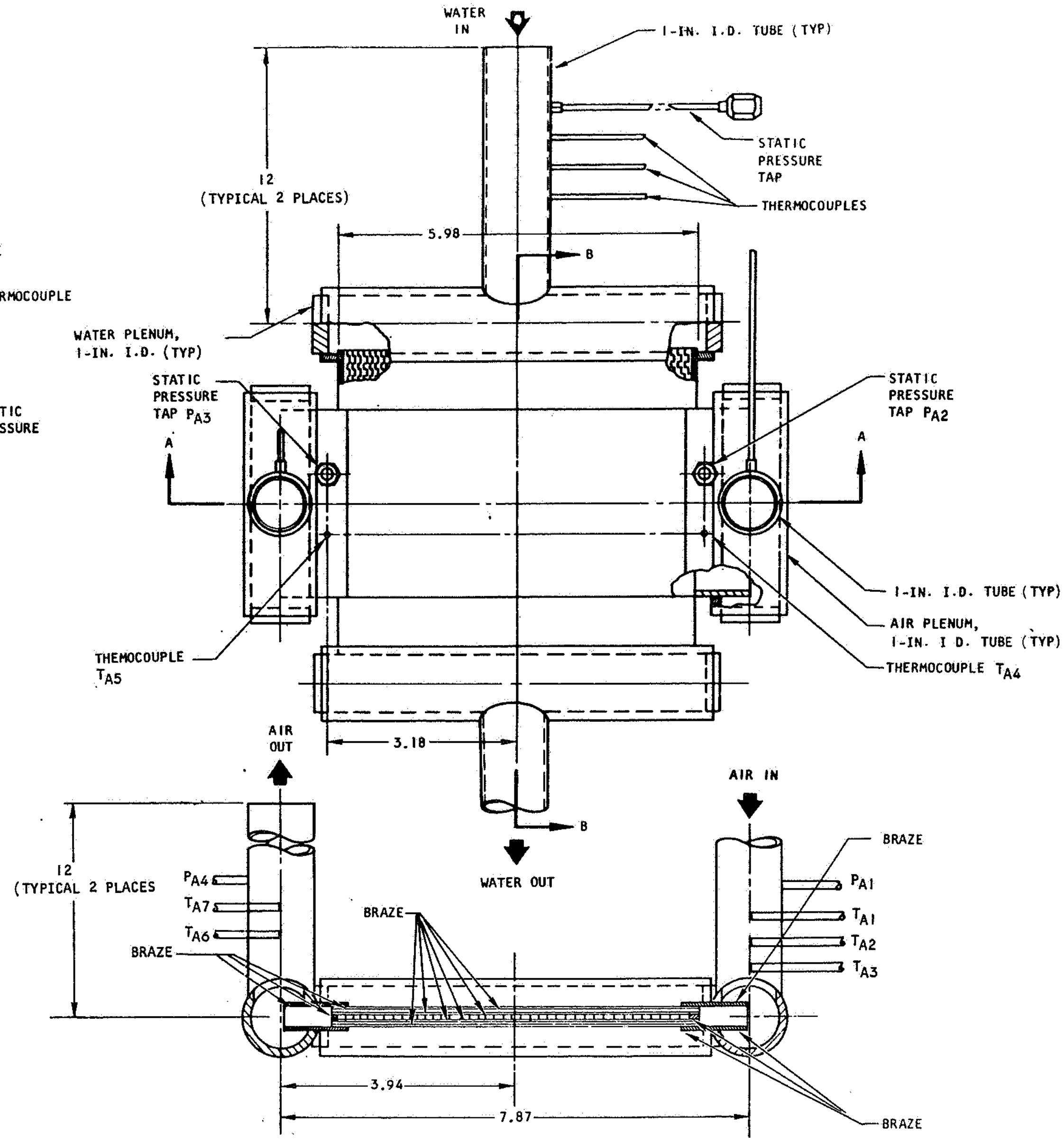

NOTES
1. PLATE-FIN SURFACES (AIR AND WATER PASSAGES) FABRICATED FROM HASTELLOY X
2. MANIFOLDING AND END CONNECTIONS FABRICATED FROM TYPE 347 CRES

L-50822

Figure 2-3. Fin Performance Test Unit

TABLE 2-1

TEST UNIT GEOMETRY

	Known Fin	Test Fins	
Fluid	water	air	air
Nominal fins-per-in. of width	20	20	28
Actual fins-per-in. of width, N	20.25	19.43	27.20
Fin height between plates (b) in.	0.075	0.050	0.050
Fin thickness (t) in.	0.004	0.006	0.006
Offset length (L_o) in.	0.100	0.100	0.100
Flow area (A) in.^{2}	0.386	0.225	0.2055
Total heat transfer area (A_T) in.^{2}	82.7	118	134
Ratio of fin area to total area, $\frac{A_f}{A_T}$	0.6068	0.746	0.794
Effective fin length (L_f) in.	0.0355	0.066	0.0593
Hydraulic diameter (d) in.	0.05584	0.0446	0.0361
Fluid flow length for heat transfer, in.	3.0	5.9	5.9
Fluid flow length for pressure drop (L) in.	-	6.0	6.0
Fluid flow width, in.	5.9	6.03	6.0
Wall thickness, in.	-	0.025	0.025
Effective wall thickness (t_w) in.	-	0.0305	0.0307
Wall conductance (t_w/kA_w) Btu/min^{0}F	-	9.65	9.45
Inlet and outlet duct flow area (A_D) in.^{2}	-	0.78	0.78
Fin effectiveness parameter ("h" is in Btu/hr-^{0}F-ft^2	$0.0943(h)^{0.5}$	$0.14(h)^{0.5}$	$0.128(h)^{0.5}$
Braze blockage width, in.	0.0	0.242	0.42
Flow area without braze blockage (A) in.^{2}	0.386	0.2345	0.221
Total heat transfer area without braze blockage (A_T) in.^{2}	82.7	123	144

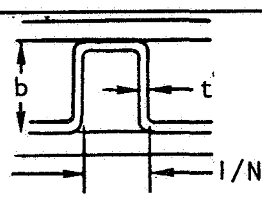

$$d = \frac{4(1/N - t)(b - t)}{2[(1/N - t) + (b - t)]}$$

3. TEST SETUP

The test unit described in Section 2 was installed in a test stand at AiResearch, Los Angeles. Figure 3-1 schematically shows the test unit installation and test instrumentation, and also the range of inlet conditions. Inlet and outlet temperatures, water temperature rise, inlet and outlet static pressures, and air and water static pressure differentials were directly measured and manually recorded. Chromel-alumel thermocouples were used in conjunction with a potentiometer for temperature measurement. Water or mercury manometers, differential-pressure bellows, and bourdon tube pressure gages were used for pressure measurement. Water flow was measured with a turbine-type flowmeter, and airflow was measured with standard laboratory airflow measuring sections utilizing sharp-edged orifices. Figures 3-2 and 3-3 depict the test setup.

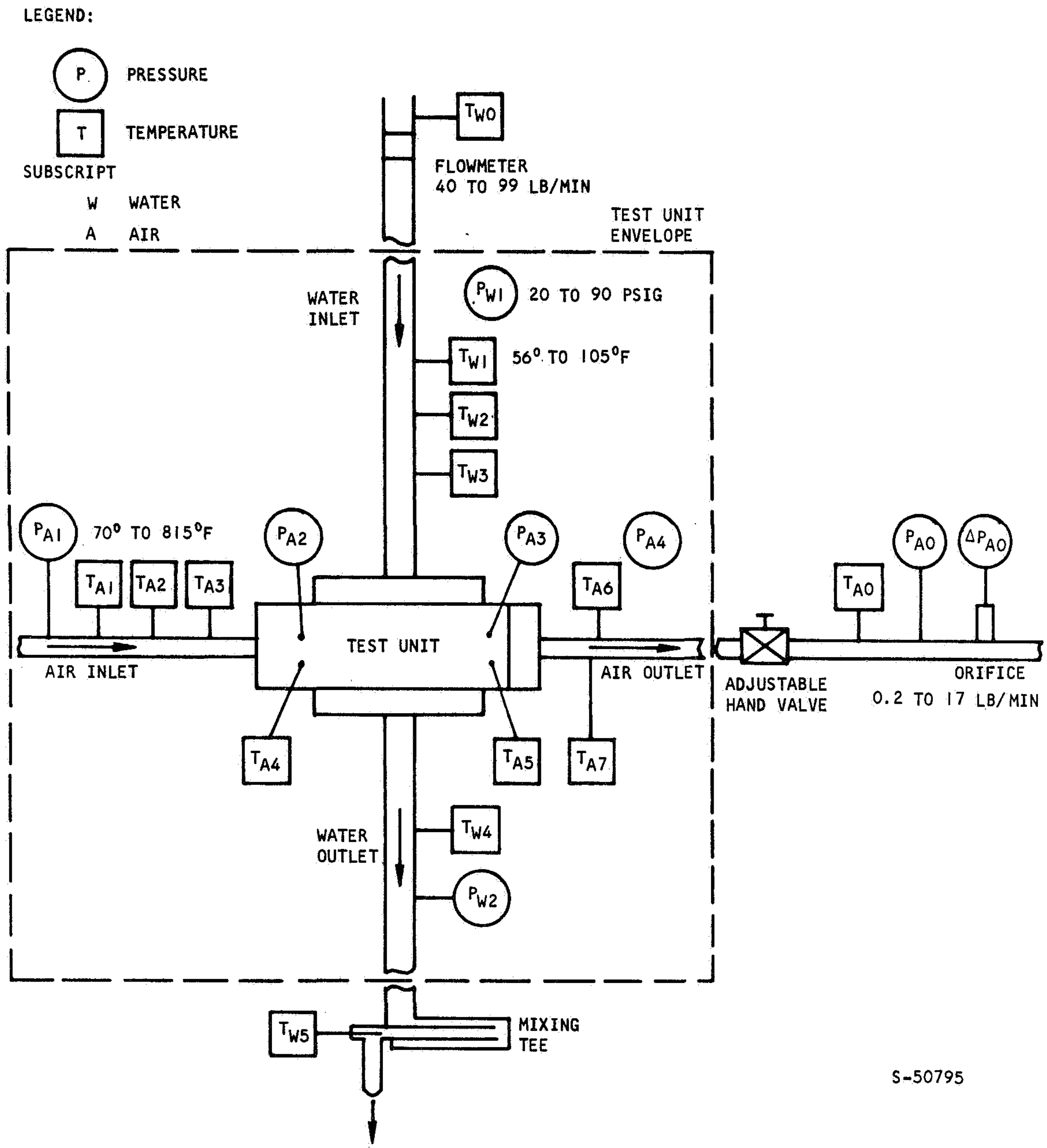

Figure 3-1. Test Setup Schematic

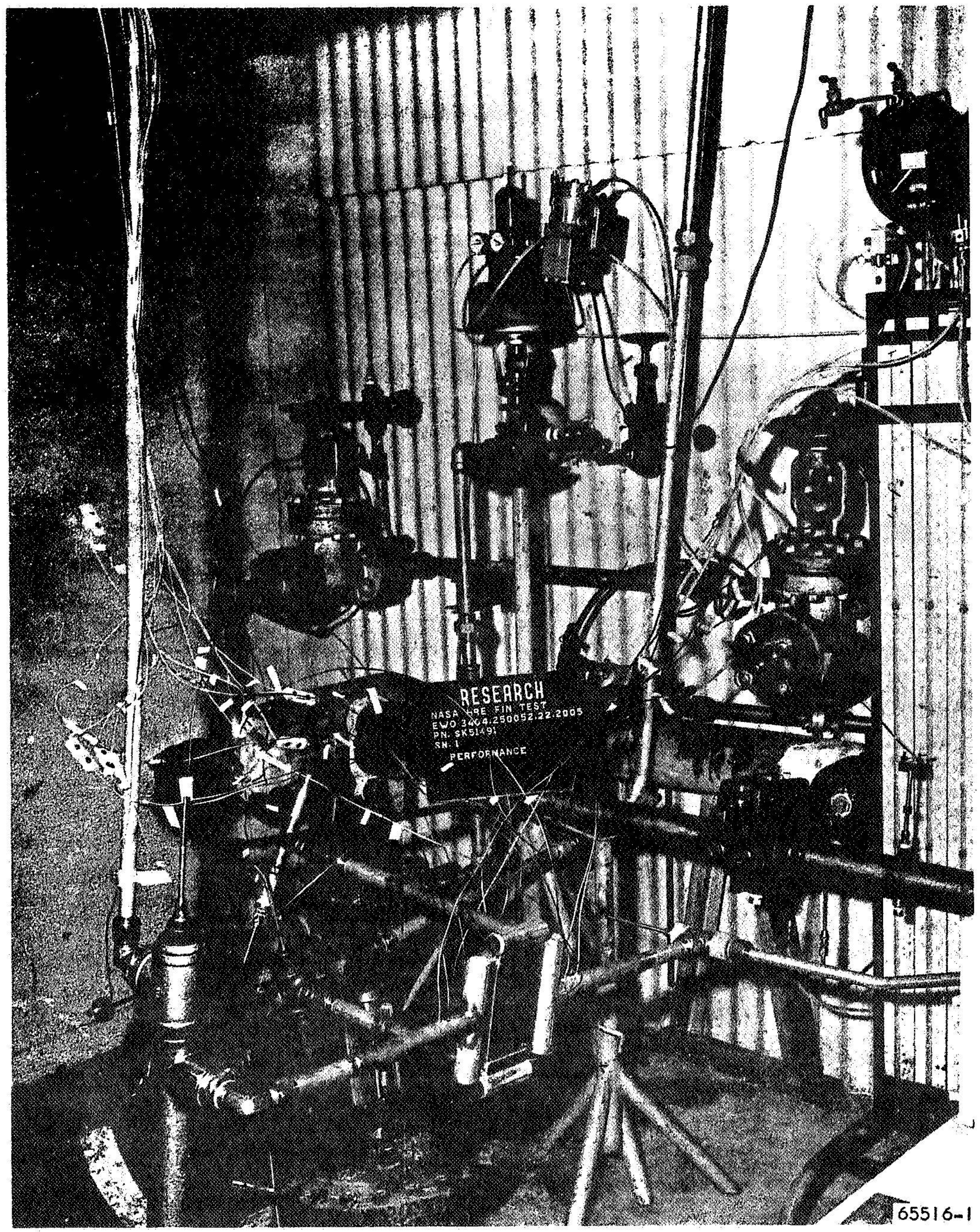

Figure 3-2. Test Setup for Fin Heat Transfer and Pressure Drop Test Before Insulation

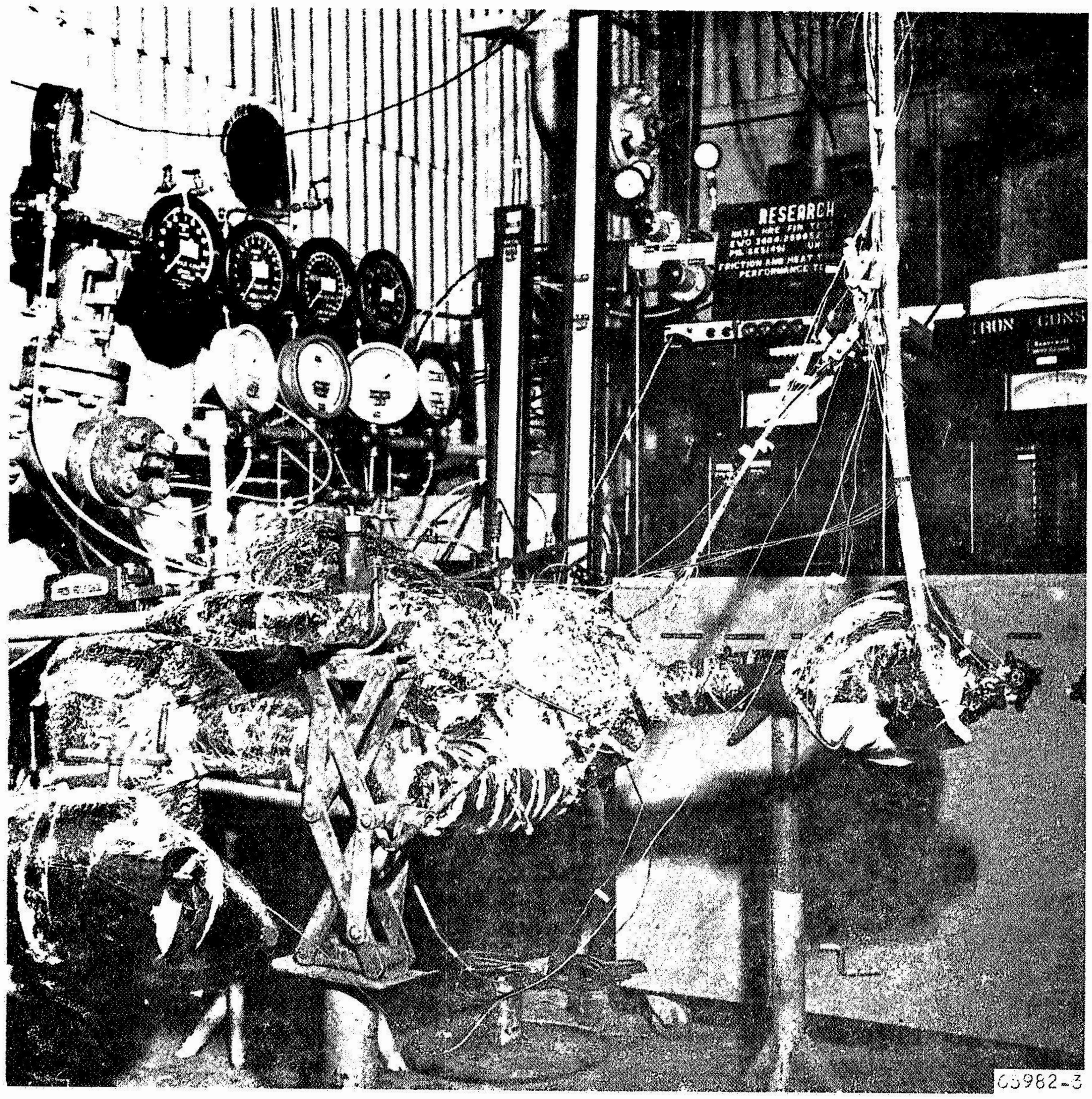

Figure 3-3. Test Setup for Fin Heat Transfer and Pressure Drop Test After Insulation

4. TEST PROCEDURE

Flows at desired inlet temperatures and pressures were established. The primary variables were hot airflow rates in the test fins, which were varied to provide a broad range of Reynolds number data. Initial system checkout tests at low water flow rates were performed to obtain a heat balance and demonstrate instrumentation consistency. A test to determine heat-leak was run with airflow at a range of inlet temperatures and flow rates commensurate with the average temperature range of tests. Isothermal pressure-drop tests were then performed with ambient temperature air in a range of flow rates. These flow rates were limited on the low side by pressure drops so small as to be incompatible with reasonable data accuracy, and limited on the high side by test unit choking at maximum test facility inlet pressure.

Data was obtained for heat transfer and pressure drop performance tests while using high temperature air at flow rates which were limited on the low side by data inaccuracy due to air-side effectiveness nearly equal to one; and on the high side by data inaccuracy due to wall- plus water-to-air-thermal conductance ratio below two, as well as by choked-flow with air at the system maximum inlet pressure. The thermal performance tests were run at a high water flow rate in order to minimize crossflow effects and sensitivity of data to uncertainties in prediction of water thermal conductance in the known fin. At intervals during the test a low water flow rate was used to provide significant water temperature changes, and to provide a check on data repeatability and instrumentation consistency in terms of a heat balance.

5. TEST RESULTS

5.1 SUMMARY OF RESULTS

The heat transfer and pressure drop performance of the nominal 20R and 28R fins are shown in Figures 5-1 and 5-2 respectively, as heat transfer factor and friction factor vs Reynolds number. For comparison, the design curves that have been used throughout the HRE analytical design work are shown. The Mach 8, 88,000-ft altitude design point Reynolds number range is from 5,000 to 46,000 for the 28R fin, and from 12,000 to 100,000 for the 20R fin. The friction factors for the 28R fin are from 70 percent to 57 percent of those used for design, while the heat transfer factors are from 97 percent to 100 percent of the design values. The friction factors for the 20R fin are from 77 percent to 73 percent of those used for design, while the heat transfer factors are from 115 percent to 130 percent of those used for design. The heat transfer factor design line is 20 percent below the test data from Figure 10-61 of Reference 5-1 fin geometry, while the friction factor design line is 20 percent above the reference test data. These margins were adopted at the program outset to accommodate the expected performance of the 6-mil-thick fins. The test data from Figure 10-61 of Reference 5-1 has a maximum Reynolds number of 3,000 for the heat transfer factor and 4,000 for the friction factor, both of which are below the design point range for the HRE. The fins for the reference test data were rectangular, with 20 fins per inch of width, a height of 125 mils between plates, and offset length of 125 mil, and were formed from 4-mil-thick nickel.

5.2 TEST DATA

Prior to collecting heat transfer and pressure drop data, heat leak, heat balance and isothermal air pressure drop data were obtained. Partially reduced heat transfer and pressure drop test data are included in Tables 5-1 and 5-2 for the nominal 20- and 28-fins-per-inch units. The indicated heat transfer rates are based on air data. To relate air data in Tables 5-1 and 5-2 to Figures 5-1 and 5-2 it is noted that for air, T_1 is the average of T_{A1}, and T_{A2}, T_2 is the average of T_{A6} and T_{A7}, P_1 is P_{A2}, and ΔP is P_{A2} minus P_{A3}. For water, T_1 is the average of T_{W1} and T_{W3}, and T_2 is T_1 minus the directly-measured difference between T_{W5} and T_{W2}.

Heat leak through the insulation to ambient air was measured in terms of air temperature drop without water flow at a near maximum airflow rate of 10 lb/min and with air inlet temperatures from 622° to 244°F. The air temperature drop was from 1.53° to 0.72°F, equivalent to from 0.4 to 0.7 percent of the temperature drop and heat transfer rate with water flow. This heat leak was not subtracted from the total heat transfer rate for any of the data analyses reported here.

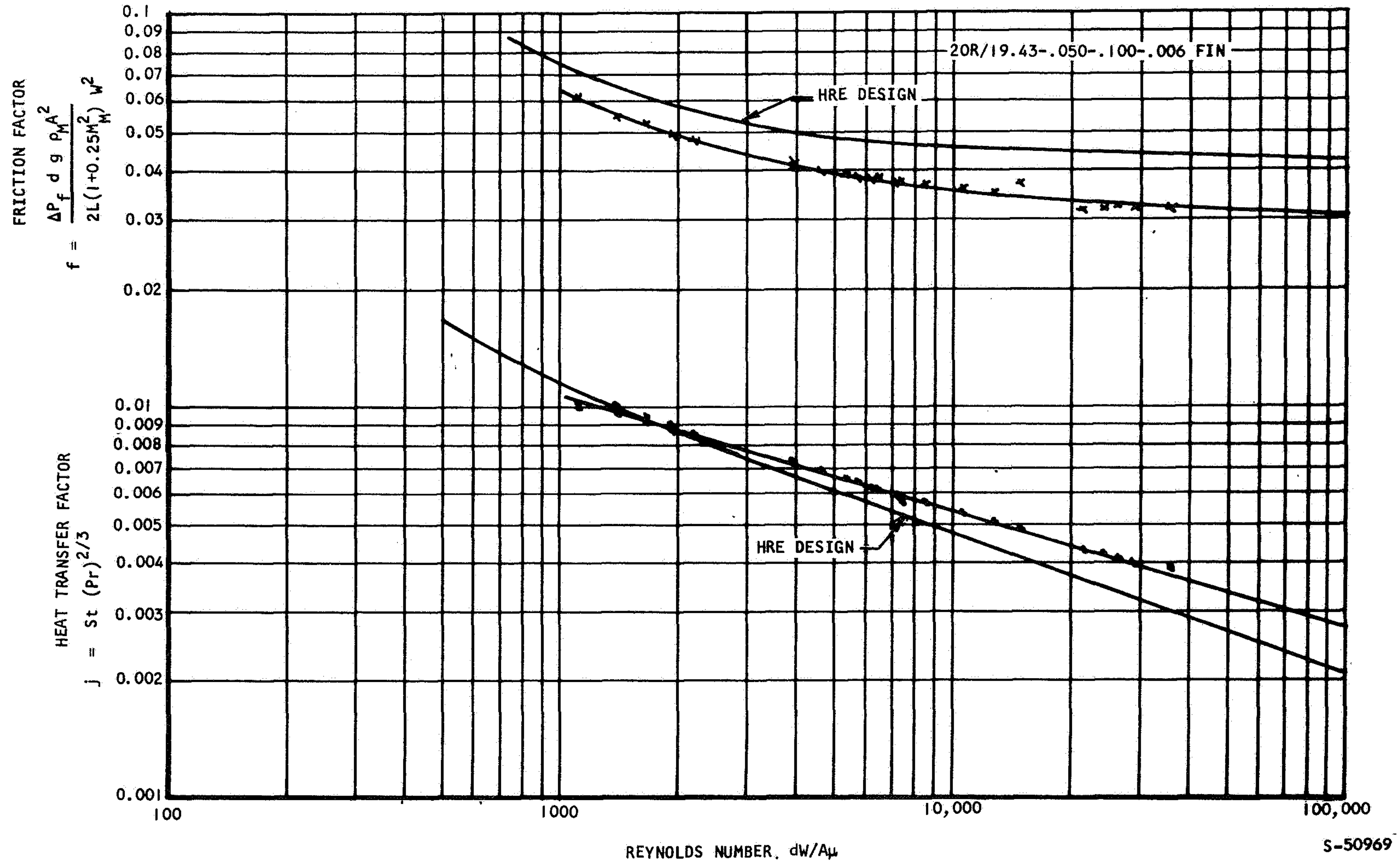

Figure 5-1. Heat Transfer and Friction Factors for 20R Fins

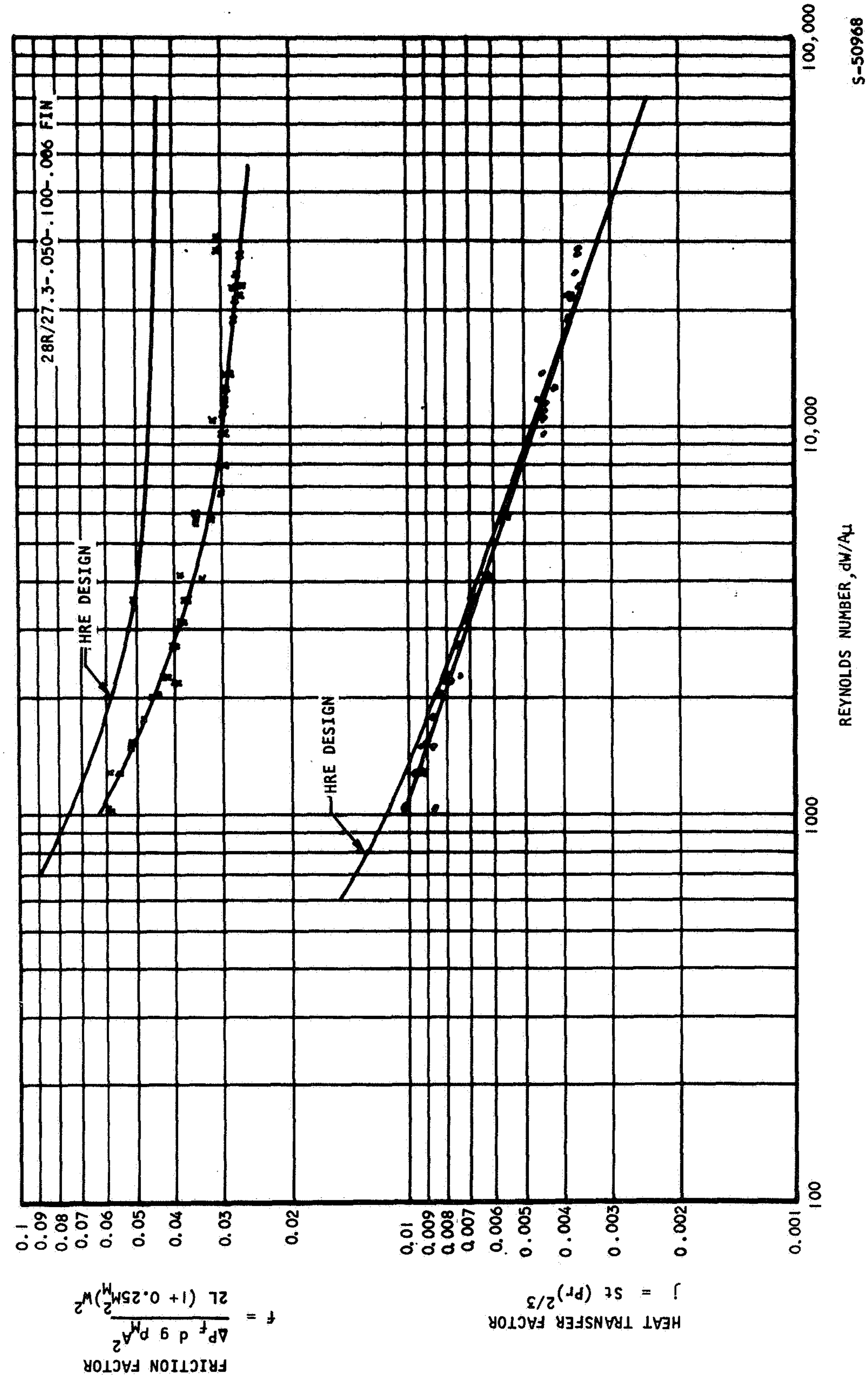

Figure 5-2. Heat Transfer and Friction Factors for 28R Fins

TABLE 5-I

HEAT TRANSFER AND PRESSURE DROP
TEST DATA FOR THE 20R FIN

Air					Water				
W, lb/min	T_1, °F	T_2, °F	P_1, in. Hg abs	ΔP_A, in. Hg	Q Btu/min	T_M, °F	W, lb/min	T_1, °F	T_2, °F
1.835	619.2	127.1	351.2	2.684	220.7	279.0	91.00	84.7	86.89
1.835	619.2	127.1	351.2	2.684	220.7	279.2	90.69	84.28	86.5
2.134	608.3	136.2	351.0	3.596	246.3	288.7	86.89	84.15	86.76
2.135	608.1	136.3	351.0	3.594	246.2	288.9	86.89	83.89	86.5
2.303	609.6	142.0	349.4	4.196	263.3	296.1	86.59	84.34	87.21
6.302	609.7	142.4	349.4	4.184	263.0	296.2	88.19	84.95	87.73
2.525	611.4	149.8	349.4	5.067	285.1	305.7	88.59	84.39	87.47
2.525	611.3	149.5	349.4	5.067	285.2	305.3	88.19	84.67	87.58
2.628	601.0	152.1	352.9	5.494	288.5	305.1	88.19	85.21	88.34
2.631	601.3	152.1	352.9	5.490	288.9	305.2	88.00	85.15	88.19
2.974	592.6	162.1	351.0	6.97	313.1	313.5	86.69	84.84	88.19
2.974	603.6	162.1	351.0	6.792	321.2	316.8	86.39	84.95	88.43
3.556	610.9	180.1	348.6	10.14	375.3	336.2	91.89	87.58	91.32
3.559	611.1	179.9	348.6	10.19	375.9	336.4	91.89	86.80	90.50
4.522	614.6	204.7	347.8	16.87	454.7	360.1	91.59	87.84	92.54
4.520	614.6	204.3	347.8	16.87	455.0	359.7	91.59	87.82	92.47
5.528	616.1	226.4	346.5	25.70	528.9	378.9	89.50	88.73	94.34
5.529	616.1	226.3	346.5	25.70	529.2	378.8	89.5	88.91	94.34
6.520	617.7	246.0	348.4	38.96	595.6	395.1	89.19	89.82	96.13
6.520	617.9	246.0	348.4	38.96	595.9	395.1	89.19	90.17	96.47
1.524	595.3	116.1	59.56	8.527	178.2	257.3	89.50	83.99	85.86
1.524	595.4	116.5	59.56	8.527	178.1	257.7	89.50	84.19	85.97
1.516	607.9	123.0	60.38	8.171	179.6	264.6	92.09	92.06	93.76
1.517	607.8	122.9	60.38	8.17	179.6	264.7	92.09	91.84	93.54
3.096	601.6	179.9	342.7	7.974	319.6	332.0	40.00	92.00	99.78
3.096	602.5	180.7	342.7	7.974	319.7	333.2	40.00	91.58	99.28
0.821	608.7	104.7	60.07	2.552	101.1	225.9	91.89	93.54	94.41
0.821	609.1	104.0	60.07	2.552	101.2	225.5	91.89	92.86	93.73

TABLE 5-I (Continued)

Air					Water				
W, lb/min	T_1, °F	T_2, °F	P_1, in. Hg abs	ΔP_A, in. Hg	Q Btu/min	T_M, °F	W, lb/min	T_1, °F	T_2, °F
0.714	602.9	100.2	60.24	1.971	87.67	216.0	92.09	91.5	92.19
0.714	601.8	100.7	60.24	1.971	87.36	214.1	92.09	92.91	93.65
0.605	594.6	96.5	60.34	1.463	73.58	204.8	92.09	90.28	90.84
0.065	594.5	96.60	60.34	1.463	73.55	202.4	91.59	91.08	91.65
0.502	536.2	103.0	60.92	1.022	52.95	191.4	91.89	99.26	99.86
0.502	579.3	103.1	60.92	1.022	58.30	196.6	91.89	99.93	100.5
0.401	578.8	101.1	60.65	.728	46.72	190.4	91.89	98.76	99.28
0.401	579.8	100.5	60.65	.728	46.88	192.8	91.89	97.99	98.52
7.778	226.2	157.5	347.3	37.73	204.3	202.5	91.00	99.26	101.49
7.775	226.6	157.7	347.3	37.73	204.6	202.8	91.19	99.34	101.5
8.906	269.8	164.1	346.3	51.20	227.5	208.5	91.59	100.1	102.7
8.906	269.8	163.9	346.3	51.20	228.0	208.4	91.19	99.93	102.5
9.617	258.6	162.7	346.9	61.40	221.4	203.1	91.19	100.3	102.9
9.619	258.3	162.8	346.9	61.40	222.0	203.4	91.19	99.60	102.2
10.57	259.0	167.3	346.6	76.09	234.4	206.6	91.19	101.5	104.3
10.57	258.6	167.0	346.6	76.09	234.1	206.2	91.19	101.3	104.0
13.14	258.9	175.4	347.6	129.3	264.9	211.8	90.59	104.8	107.7
13.14	258.9	175.4	347.6	129.3	265.2	211.9	90.59	103.3	106.2

TABLE 5-2

HEAT TRANSFER AND PRESSURE DROP
TEST DATA FOR THE 28R FIN

Air					Water				
W, lb/min	T_1, °F	T_2, °F	P_1, in. Hg abs	ΔP_A, in. Hg	Q Btu/min	T_M, °F	W lb/min	T_1, °F	T_2, °F
11.18	251.3	146.8	343.3	108.5	282.2	191.5	92.4	73.29	77.61
11.18	251.3	147.2	343.3	108.5	281.2	191.7	93.5	73.70	76.90
8.780	251.6	136.2	344.9	60.5	244.7	184.3	93.5	71.31	73.98
8.773	254.4	136.7	344.7	60.58	249.2	183.6	93.5	72.18	75.13
8.524	250.0	135.7	344.3	59.93	235.1	183.1	92.00	73.02	75.77
8.518	250.0	135.5	343.7	57.93	235.4	183.0	92.00	73.56	75.81
7.589	251.3	131.2	345.7	45.38	220.1	180.3	92.25	72.61	75.42
7.595	251.3	131.0	345.7	45.38	220.6	180.3	92.25	71.54	74.27
6.579	590.7	219.8	342.9	46.06	611.5	369.4	90.50	77.4	84.0
6.584	599.8	219.7	342.9	44.67	613.9	369.8	90.50	76.6	83.39
5.567	603.9	201.2	344.7	31.62	549.6	356.2	90.39	74.11	80.91
5.567	606.0	201.4	344.7	31.62	552.1	357.3	90.39	73.22	79.88
4.487	597.4	183.3	346.7	19.68	454.9	339.2	85.56	70.72	76.84
4.473	597.4	176.0	346.7	19.58	461.5	332.3	85.39	71.29	77.24
3.630	595.3	151.0	346.7	12.24	394.2	308.2	94.5	68.81	73.49
3.630	595.4	151.2	346.7	12.24	394.2	308.3	93.79	68.79	73.77
3.041	591.8	134.6	348.4	8.466	339.6	290.1	92.19	67.06	72.34
2.691	589.6	125.6	347.8	7.533	304.79	278.6	93.19	68.24	72.77
2.691	589.9	125.3	347.8	7.533	305.2	278.2	93.19	68.31	72.97
2.589	598.9	122.8	348.4	6.982	300.9	277.6	92.19	68.24	71.77
2.588	599.8	123.0	348.4	6.982	301.3	278.0	92.19	68.47	71.97
2.519	595.5	120.3	345.9	6.315	292.2	273.6	92.00	68.27	71.84
2.519	604.4	120.4	345.9	6.615	297.7	277.1	91.79	66.45	70.04
1.788	590.1	97.44	348.8	3.439	214.8	241.5	86.39	65.5	68.13
1.788	590.1	96.73	348.8	3.439	215.1	240.6	86.39	65.27	67.86
1.509	583.3	86.73	61.2	10.30	182.6	222.0	85.00	64.8	67.27
1.509	583.3	87.59	91.2	10.30	182.3	222.8	85.0	65.49	67.81
1.524	598.7	83.7	61.2	10.36	191.3	223.9	90.59	61.09	63.68

TABLE 5-2 (Continued)

Air					Water				
W, lb/min	T_1, °F	T_2, °F	P_1, in. Hg abs	ΔP_A, in. Hg	Q Btu/min	T_M, °F	W, lb/min	T_1, °F	T_2, °F
1.524	598.5	87.82	61.20	10.36	190.9	224.6	90.59	62.18	64.54
1.318	593.4	79.34	61.20	7.658	165.1	213.12	91.79	61.54	63.54
1.318	593.4	77.86	61.20	7.658	165.1	212.8	91.79	61.95	63.97
1.119	588.1	72.87	61.20	5.563	140.5	198.2	98.89	60.54	62.13
1.119	588.1	72.83	61.2	5.563	140.5	198.7	98.89	60.18	61.90
0.920	580.9	66.90	61.60	3.836	115.2	187.7	91.39	56.63	58.47
0.809	572.7	63.06	61.20	3.072	100.3	171.1	89.00	57.27	58.77
0.809	572.4	62.93	61.20	3.072	100.3	172.3	89.00	56.81	57.79
0.594	581.2	72.92	60.99	1.947	73.61	166.8	90.59	70.61	71.5
0.594	581.1	73.46	60.99	1.947	73.51	171.1	90.59	70.24	71.18
0.502	570.5	72.78	60.99	1.455	60.85	159.8	90.00	71.29	72.24
0.502	570.3	72.19	60.99	1.455	60.90	157.9	90.00	70.77	71.68
12.35	234.0	139.1	365.5	148.9	282.7	180.4	91.29	59.56	62.36
11.35	232.5	132.5	375.7	114.4	274.2	175,4	89.29	59.84	62.68
11.35	232.4	132.4	375.7	114.2	274.6	175.3	89.29	59.84	62.59
9.949	249.6	133.9	347.8	80.57	277.8	182.8	91.75	60.04	62.63
9.947	249.8	134.0	347.8	80.57	278.2	182.9	91.75	60.04	62.70
8.523	249.6	127.8	349.8	56.91	250.5	178.4	91.75	60.09	62.86
8.523	249.6	128.1	349.8	56.91	249.8	178.7	91.75	59.90	62.68
7.583	249.3	122.8	347.8	22.19	231.5	174.7	91.00	59.63	61.93
7.583	249.5	122.7	347.8	22.19	231.9	174.7	91.29	59.59	62.18
1.520	596.3	83.69	58.75	10.56	189.9	223.0	90.00	61.31	63.56
1.526	596.3	84.75	58.75	10.56	189.5	225.0	90.00	61.31	63.52
1.320	593.1	79.24	58.95	8.00	165.2	212.9	88.69	61.52	63.47
1.32	593.1	79.53	58.95	8.00	165.2	212.6	88.69	62.22	63.72
1.120	587.8	74.90	56.50	6.027	139.9	199.9	88.69	62.40	64.11
1.12	587.8	75.21	56.91	6.027	139.8	200.8	88.69	62.29	64.06
0.923	591.6	68.65	57.93	4.130	117.6	187.8	89.19	59.90	61.38
0.923	592.7	68.33	58.13	4.138	118.0	186.4	89.19	60.09	61.45

TABLE 5-2 (Continued)

Air							Water		
W, lb/min	T_1, °F	T_2, °F	P_1, in. Hg abs	ΔP_A, in. Hg	Q Btu/min	T_M, °F	W, lb/min	T_1, °F	T_2, °F
0.812	591.1	67.51	58.24	3.381	103.5	180.2	89.79	61.04	62.36
0.825	591.0	67.27	58.24	3.381	105.2	179.5	89.19	61.04	62.31
0.706	589.6	64.86	58.34	2.638	90.31	170.2	89.19	60.5	61.77
0.706	590.2	65.04	58.34	2.638	90.38	170.3	89.19	60.8	61.90
0.609	584.1	63.27	58.54	2.065	77.26	162.0	88.69	60.22	61.45
0.609	584.1	63.22	58.54	2.065	77.26	162.8	88.69	60.20	61.27
0.504	579.9	61.86	57.12	1.624	63.56	155.3	86.5	59.80	60.52
0.504	579.5	61.45	57.12	1.624	63.56	153.7	86.5	59.7	60.4
0.403	574.0	60.99	59.15	0.998	50.31	141.6	87.5	60.29	60.95
1.800	615.9	118.6	346.3	3.189	218.7	264.8	89.19	85.73	88.26
1.800	615.9	118.4	346.3	3.189	218.8	264.4	89.50	85.78	88.21
3.63	615.3	143.6	346.0	6.776	303.7	298.3	88.00	87.00	90.39
9.464	610.4	288.3	347.0	106.8	759.8	420.8	92.09	93.65	102.13
9.464	608.9	283.0	347.0	106.8	759.1	419.3	92.09	93.30	101.7
11.62	612.0	310.6	345.1	203.9	863.8	439.8	90.89	93.99	103.5
11.62	612.0	310.4	345.1	203.9	864.1	439.6	90.89	94.52	104.04
0.913	598.9	91.69	59.77	3.785	113.00	205.5	92.09	83.82	85.0
0.913	598.8	91.47	59.77	3.785	113.0	204.9	92.09	83.82	85.00
0.911	604.3	91.78	59.26	3.711	113.9	207.7	91.29	83.47	84.56
0.911	603.5	91.58	59.26	3.822	113.8	205.1	91.29	84.17	85.26
9.586	275.9	159.3	346.7	75.071	207.0	208.5	90.5	86.4	86.28
9.570	275.4	159.2	346.7	75.07	268.6	208.2	90.5	86.28	89.06
5.519	422.9	172.2	347.2	27.53	336.1	269.6	90.00	87.7	91.34
5.519	422.9	172.8	347.2	27.53	335.4	270.2	90.00	87.71	91.23
5.506	616.4	218.7	346.7	31.41	537.5	372.3	89.00	90.17	96.00
5.506	616.7	218.4	346.7	31.41	538.3	372.1	89.00	90.60	96.43
5.470	815.3	267.9	344.7	37.94	745.1	478.9	88.50	93.52	101.9
5.470	814.6	268.6	344.7	37.94	743.3	479.3	88.50	93.26	101.6

Heat balance was determined before and intermittently during test with a nominal water flow of 6 lb/min at 50^0 to 93^0F inlet temperature for air flows of 3 lb/min at 600^0F inlet temperature and 14 lb/min at 210^0F inlet temperature. The water temperature rise was about 50^0F at 3 lb/min and 35^0F at 14 lb/min. Heat balance is defined as 100 $(Q_W - Q_A)/Q_A$. The ranges of heat balances for the 28-fin unit were -1.15 percent to 4.75 percent at 3 lb/min, and -3.43 percent to -4.81 percent at 14 lb/min. For the 20-fin unit, heat balances were from -1.15 percent to 1.82 percent at 3 lb/min air flow rate, run with a water flow rate of 6 lb/min.

Isothermal pressure drop data is presented as a dimensionless correlation of Fanning friction factor vs Reynolds number in Figure 5-3. The range of ambient temperature air flow rate was from 0.2 to 15 lb/min for both units.

The use of water flow rates from 85 to 100 lb/min in the known fin resulted in water-to-air thermal conductance ratios from 6.9 to 42 for the 20R test fin, and from 5.55 to 30.2 for the 28R test fin. The low wall-thermal conductance produced by the combined 25-mil-thick Hastelloy X walls and the 6-mil-thick fin roots reduced the combined wall plus water-to-air thermal conductances ratios to the range from 1.81 to 11.23 for the 20R test fin and from 1.74 to 9.64 for the 28R test fin.

5.3 DATA ANALYSIS AND DISCUSSION

Heat transfer and pressure drop performance was reduced to relations between dimensionless parameters, as plotted in Figures 5-1 through 5-3. The data analysis procedure is summarized below:

Air Reynolds number in the test fin is defined as $Re = \frac{dW}{A\mu}$ (5-1)

where d and A are as in Table 2-1, μ is evaluated at log mean average bulk temperature from Figure 5-4, and W is the measured air flow rate.

Log mean average bulk air temperature is

$$T_M = \frac{T_{W1} + T_{W2}}{2} + \Delta T_{LM} \qquad (5\text{-}2)$$

where ΔT_{LM} is the log mean difference between air and water temperatures calculated for crossflow with both fluids unmixed in the fins and completely mixed in the manifolds by the method of Reference 5-2.

Friction pressure drop is obtained from overall static pressure drop by subtracting calculated pressure drop due to entrance contraction, exit expansion and change in flow momentum. The ratio of $\Delta P_f/\Delta P$ was always above 0.91.

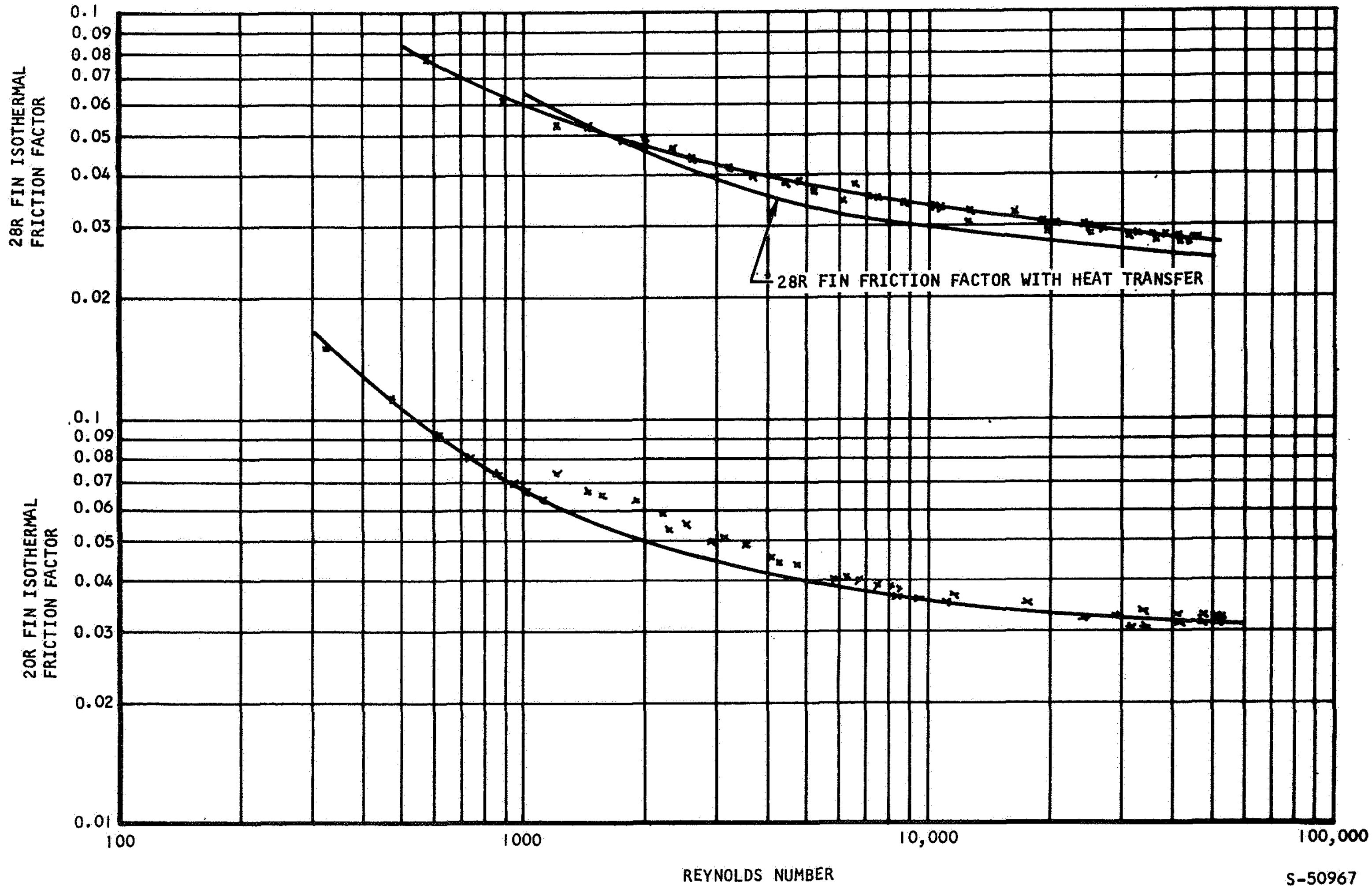

Figure 5-3. Isothermal Friction Factor for 20R and 28R Fins

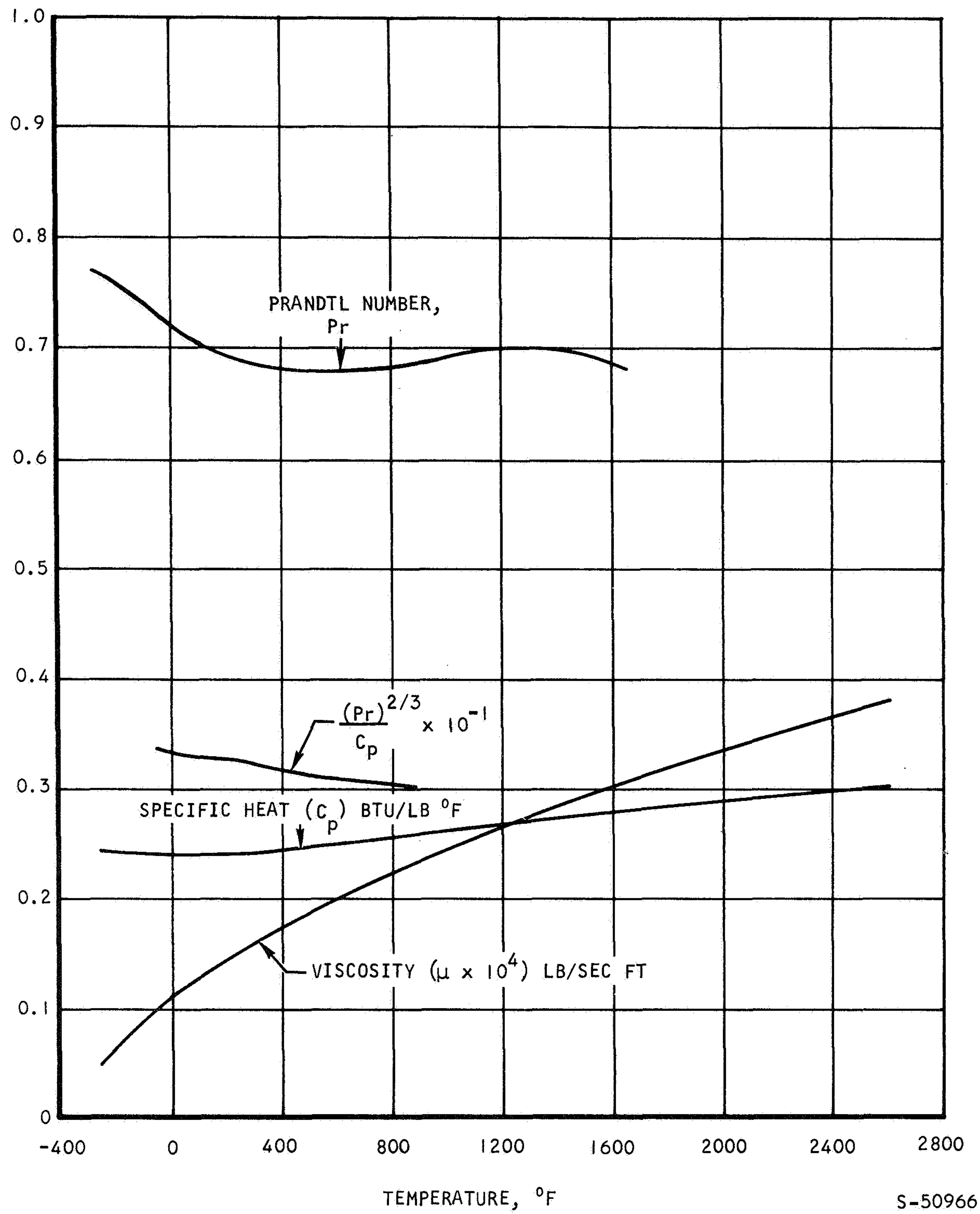

Figure 5-4. Air Properties

$$\Delta P_f = \Delta P - \frac{W^2}{A^2 2g}\left(\frac{(1 + .25\ M_1^2)K_1}{\rho_1} + \frac{(1 + .25\ M_2^2)K_2}{\rho_2} + \left(1 + \left(\frac{A}{A_D}\right)^2\right)\left(\frac{1 + .25\ M_2^2}{\rho_2} - \frac{1 + .25\ M_1^2}{\rho_1}\right)\right) \quad (5\text{-}3)$$

where entrance contraction loss coefficient, K_1, = 0.5 and exit expansion loss coefficient, K_2, = 0.49 for the 20R fin, and 0.52 for the 28R fin. The Mach number function, $(1 + .25\ M^2)$, is an approximation to the isentropic compressible flow effect. The maximum error in the approximation is 2.5 percent at Mach 1. Mach number, M, is calculated at measured local inlet and outlet temperature and pressure and with core flow area, A. The indicated densities, ρ, are calculated at measured inlet and outlet conditions by the perfect gas equation.

$$\rho = \frac{P}{RT} \quad (5\text{-}4)$$

Fanning friction factor is obtained from

$$f = \frac{\Delta P_f\ d\ 2\ g\ \rho_M\ A^2}{4\ L\left(1 + .25 M_M^2\right) W^2} \quad (5\text{-}5)$$

where the static density, ρ_M, is evaluated at arithmetic average absolute pressure and log mean average absolute temperature by

$$\rho_M = \frac{P_1 - (\Delta P/2)}{R\ T_M} \quad (5\text{-}6)$$

The heat transfer factor for the test fin was calculated from overall test thermal conductance, UA, and calculated thermal conductance for the known fin with water, $(\eta_o\ hA)_w$, as based on test performance with air.

Overall performance was calculated from

$$UA = \frac{W\ C_p\ (T_1 - T_2)}{\Delta T_{LM}} \quad (5\text{-}7)$$

where the air specific heat, C_p, was evaluated at the average of T_1 and T_2 from Figure 5-4. The log mean temperature difference, ΔT_{LM}, for cross flow, was calculated by the method of Reference 5-2. Since the water temperature rise was so low, the log mean temperature difference was not more than 2 percent below the counterflow-log mean temperature difference.

The thermal conductance for water flowing in the known fin was calculated with geometry from Table 2-1 by

$$\left(\eta_o\ h\ A_T\right)_w = \eta_f\ h\ A_f + h\ (A_T - A_f) \tag{5-8}$$

where

$$h = \frac{j\ W\ C_p}{A(Pr)^{2/3}} \tag{5-9}$$

with j obtained from Figure 5-5 at water $Re = \frac{dW}{A\mu}$

and C_p, Pr, and μ of water obtained from Figure 5-6 at arithmetic average water temperature.

The effectiveness of the known fin, η_f, was calculated by

$$\eta_f = \frac{\tanh \left(\frac{2\ h}{k\ t}\right)^{0.5} L_f}{\left(\frac{2\ h}{k\ t}\right)^{0.5} L_f} \tag{5-10}$$

where $(2\ h/k\ t)^{0.5}\ L_f$ is called fin effectiveness parameter and is noted in Table 2-1 as a function of heat transfer coefficient.

The thermal conductance for air in the test fin was calculated from overall conductance, water conductance in the known fin, and wall conductance by,

$$(\eta_o\ h\ A_T)_A = \frac{1}{\frac{1}{UA} - \frac{1}{(\eta_o\ h\ A_T)_W} - \frac{t_w}{k\ A_w}} \tag{5-11}$$

where wall thermal conductance, $t_w/k\ A_w$ is noted in Table 2-1.

The test fin heat transfer coefficient was calculated with geometry and fin effectiveness parameters from Table 2-1 by iterating with

$$h = \frac{(\eta_o\ h\ A_T)_A}{\eta_f\ A_f + A_T - A_f} \tag{5-12}$$

where

$$\eta_f = \frac{\tanh \left(\frac{(2t + 2\ L_o)h}{k\ t\ L_o}\right)^{0.5} L_f}{\left(\frac{(2t + 2\ L_o)h}{k\ t\ L_o}\right)^{0.5} L_f} \tag{5-13}$$

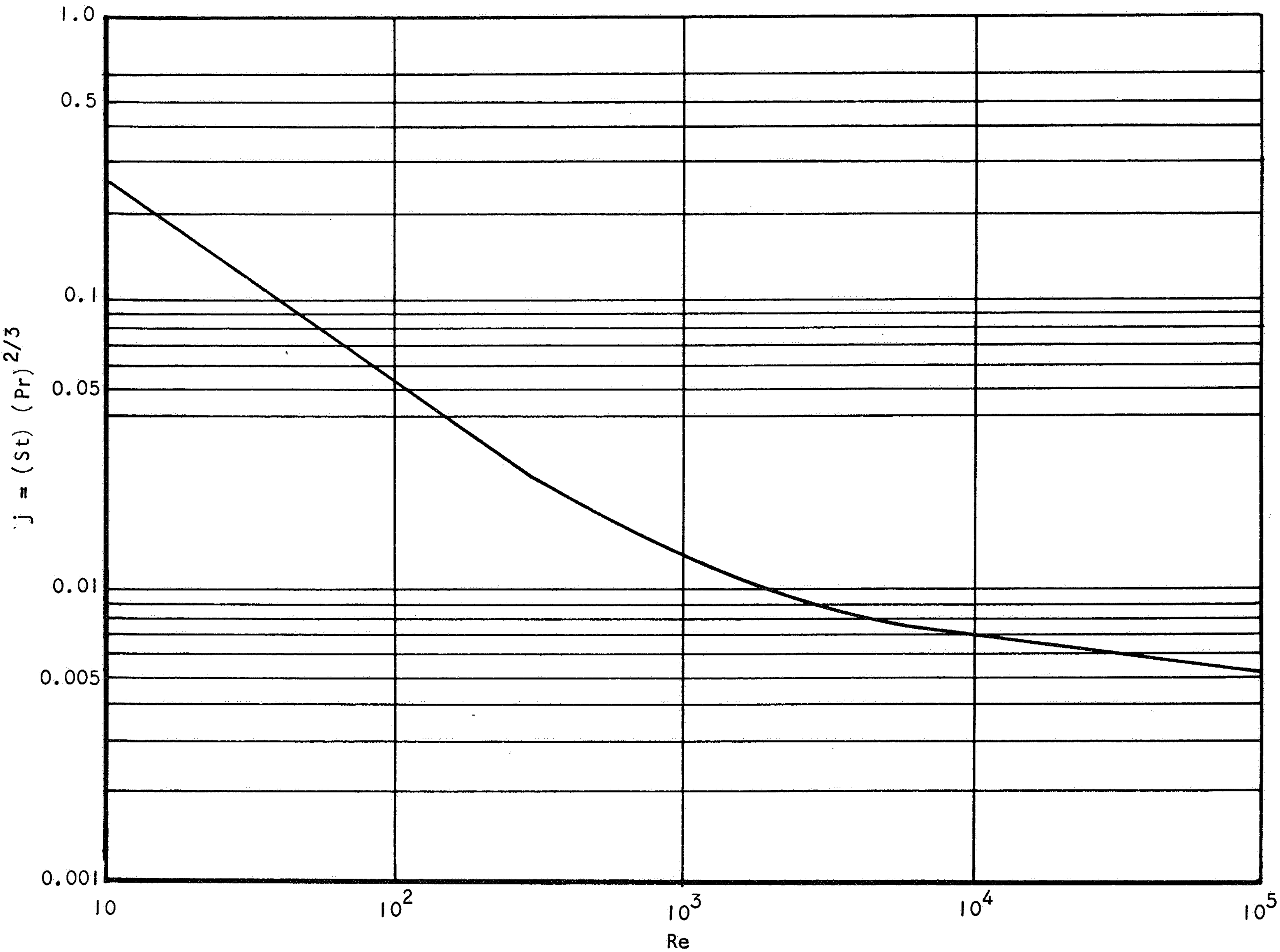

Figure 5-5. Heat Transfer Factors for Known Fin

S-50821

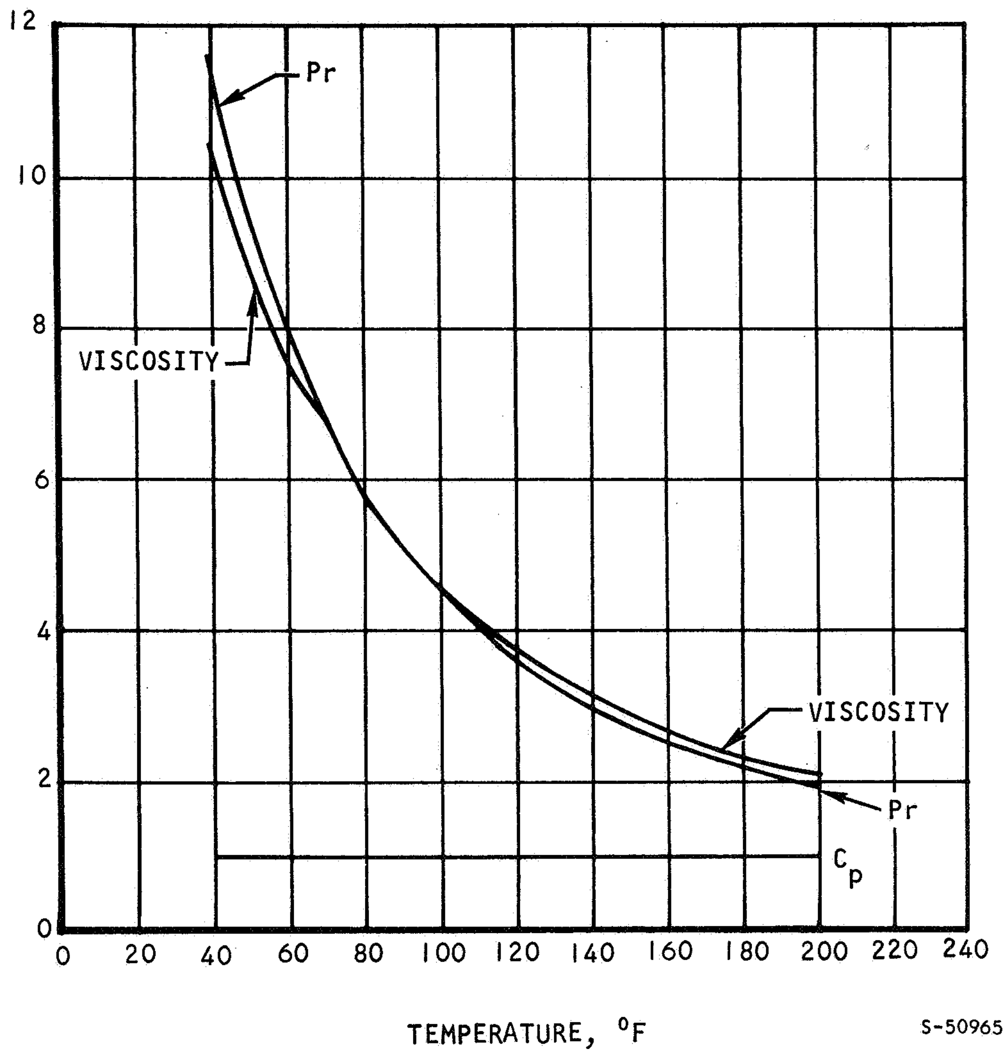

Figure 5-6. Water Properties

The heat transfer factor, j, was calculated with test fin air-flow area from Table 2-1 by

$$j = St\,(Pr)^{2/3} = \frac{h\,A\,(Pr)^{2/3}}{C_p\,W} \qquad (5\text{-}14)$$

and the fin effectiveness parameter is noted in Table 2-1 as a function of heat transfer coefficient.

6. CONCLUSIONS

Basic flow friction and heat transfer data is now available for the fins used in the high heat flux areas and large pressure drop zones of the regeneratively cooled HRE shells. Based on this data, the fin friction pressure drop for the HRE should be as much as 25 percent below the values calculated during the program. The calculated cross-section temperature difference remains at $930^{\circ}R$ for the peak heat flux of 700 Btu/sec ft^2 at the Mach 8, 88,000-ft altitude design condition.

REFERENCES

5-1 Kays, W.M., and A.L. London, Compact Heat Exchangers, Second Edition, McGraw-Hill, New York, 1964.

5-2 Mason, J.L., "Heat Transfer in Cross Flow" Proceedings of the Second U. S. National Congress of Applied Mechanics, ASME, N. Y., 1955, p 801.